<u>Citation:</u> Basereh, S., Okumus, P., Aaleti, S. (2020). "Seismic Retrofit of Reinforced Concrete Shear Walls to Ensure Reparability.", ASCE SEI Congress, April 5-8, St Louis, MO, 498-509, https://doi.org/10.1061/9780784482896.046.

Seismic retrofit of reinforced concrete shear walls to ensure reparability

Sina Basereh¹; Pinar Okumus, Ph.D.²; Sriram Aaleti, Ph.D.³

¹Ph.D. Candidate, Department of Civil, Structural and Environmental Engineering, University at Buffalo, State University of New York, Buffalo, NY 14260. Email: sinabase@buffalo.edu

²Associate Professor, Department of Civil, Structural and Environmental Engineering, University at Buffalo, State University of New York, Buffalo, NY 14260. Email: pinaroku@buffalo.edu

³Associate Professor, Department of Civil, Construction and Environmental Engineering, University of Alabama, Tuscaloosa, AL 35487. Email: saaleti@eng.ua.edu

ABSTRACT

Many reinforced concrete (RC) buildings built before the adoption of modern seismic codes in high seismic regions need to be retrofitted to perform well in a major earthquake. This study introduces a new retrofit method for code-deficient reinforced concrete shear walls that are vulnerable to non-ductile failure modes due to improper detailing or lack of well-confined boundary elements. The retrofit method combines weakening of shear walls with a base cut and self-centering of the walls with the addition of external unbonded post-tensioned strands. The retrofitted walls are expected to have controlled rocking behavior as opposed to the original walls that undergo shear and flexure and are expected to have minimized damage caused by earthquakes resulting in shorter repair times and lower repair costs.

Three-dimensional finite element models of pre- and post-retrofit shear walls under cyclic lateral loading were used to identify working details of the retrofit method. To transfer shear at base and minimize shear slip, shear keys and other non-straight wall base cut shapes were explored. The contribution of shear, flexure and rocking to the global response were measured and compared for pre- and post-retrofit walls. Results of analysis showed that rocking is the governing behavior for the retrofitted walls and contribution of shear to displacements decreased due to retrofit. Changes in residual displacements, energy dissipation, strength and secant stiffness due to retrofit were documented.

INTRODUCTION

Past earthquakes have shown that buildings with reinforced concrete (RC) walls that are not compliant with modern seismic codes can undergo severe damage. Shear-dominated failure modes in the form of diagonal tension, diagonal compression, or sliding shear were documented for these non-ductile buildings (Kam and Pampanin 2011; Wallace 2012). To retrofit buildings with damage-prone RC walls, combination of selective weakening and self-centering in the form of rocking is proposed.

Self-centering is the ability of a system to return to the plumb upon unloading to minimize residual drift and consequently, damage. Gravity or use of bonded or unbonded post-tensioning strands can provide self-centering. This study is focused on controlled rocking with unbonded post-tensioning as a self-centering mechanism. One of the very first studies of self-centering was conducted in the Precast Seismic Structural Systems (PRESSS) program. In the PRESSS program, a building with self-centering precast frame in one direction and jointed rocking wall system in the orthogonal direction was investigated. Low energy dissipation capacity of the rocking wall system was improved with U-shaped flexure plates (UFP) to connect wall panels (Nakaki et al. 1999; Priestley et al. 1999; Priestley and Tao 1993). Following the PRESSS program, rocking precast RC shear walls emerged as a new design solution for regions of medium to high seismic risk. Many researchers have investigated different rocking wall configurations, namely, single rocking walls (Kurama et al. 1999; Nazari et al. 2017; Perez et al. 2004; Sharma and Aaleti 2019), jointed rocking walls (Aaleti and Sritharan 2009; Sritharan et al. 2007), and precast walls with end columns (PreWEC) with various energy dissipation mechanisms (Aaleti and Sritharan 2011; Sritharan et al. 2015; Twigden et al. 2017). Mild steel energy dissipaters in the form of low yield strength tapered longitudinal reinforcement or dog-bone shaped mild reinforcing bars connecting the wall to the foundation (Holden et al. 2003; Rahman and Restrepo 2000; Restrepo and Rahman 2007; Smith and Kurama 2014; Smith 2012; Smith et al. 2010), O-shaped connectors between wall panels (Henry 2011; Henry et al. 2010; Twigden and Henry 2015), and viscous dampers (Kurama 2000) were used for energy dissipation and damping.

Selective weakening is an intervention through which, selected elements of a system are weakened or removed to reduce strength and/or stiffness. Generally, weakening results in lower force demand on the system together with increased displacement demand. To accommodate additional displacement demands and to ensure minimized damage, external confining mechanisms, damping mechanisms, advanced cementitious materials, or jacketing may be provided (Kam and Pampanin 2008; Kam and Pampanin 2010; Pampanin 2006; Yang and Okumus 2017; Yang et al. 2019). Ireland et al. (2007) selectively weakened RC shear walls through vertical and/or horizontal straight base cut and used external energy dissipaters to investigate the strength and residual drift of the retrofitted walls.

The current study combines self-centering and weakening concepts and applies them to non-ductile RC shear walls. Weakening is accomplished by making a full, non-straight cut at wall base and self-centering is enabled by using external unbonded post-tensioning strands to walls. Three-dimensional finite element analysis (FEA) was used as a tool to first, model a code-deficient RC shear wall and second, implement the proposed retrofit solution. A parametric study was conducted to understand the effect of varying cut shapes on the global response of retrofitted walls. Energy dissipation capacity, lateral strength, residual displacement, secant stiffness, principal strain contours of pre- and post-retrofit walls are compared. Deformation decomposition of the original and retrofitted walls is presented as an indicator for failure mode change.

BENCHMARK RC WALL

A slender (i.e. height-to-length ratio of 2 or more) RC shear wall tested by Pilakoutas and Elnashai (1995) was selected as a benchmark wall for FEA. The wall specimen, SW6, was tested under

lateral cyclic loading up to the failure. Elevation and cross section views of the wall are shown in **Figure 1**. Although web of the selected wall was compliant with the requirements of ACI 318-14 (ACI 2014) in terms of vertical and transverse reinforcement ratio, the wall is categorized as non-code-compliant since it did not meet the requirements of ACI 318-14 (ACI 2014) for special boundary elements. The height of the special boundary element, vertical spacing of confining reinforcement in the boundary element, and extension of boundary element to the foundation were not compliant with the requirements of ACI 318-14 (ACI 2014). Failure of the wall was due to concrete crushing in the web and boundary element together with the fracture of transverse reinforcement, which led to the flexure-shear failure mode. More details about the wall can be found elsewhere (Pilakoutas and Elnashai 1995).

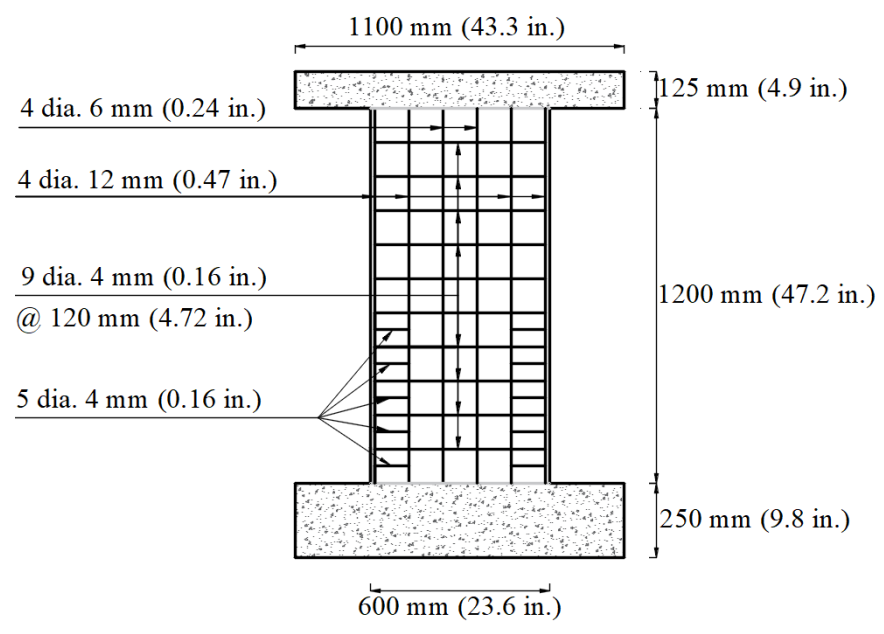


Figure 1. Elevation view of the pre-retrofit wall (SW6)

FEA of the wall

RC shear wall was modeled using a general-purpose nonlinear finite element package, LS-DYNA (LSTC 2017). Concrete was modeled using the smeared crack, Winfrith material model (MAT 084 in LS-DYNA) which is suitable to model concrete under cyclic and/or seismic actions (Bruneau et al. 2018; Epackachi and Whittaker 2018). Winfrith material model requires modulus of elasticity, uniaxial compressive and tensile strength, aggregate size, and crack width at which crack-normal tensile stress drops to zero. Uniaxial compressive strength of concrete was 38.6 MPa (5.6 ksi) and maximum aggregate size was 10 mm (0.4 in.). Tensile strength of concrete was calculated using the lower bound threshold of fib model code (fib 2013), post-peak tensile behavior was approximated as linear, and modulus of elasticity of concrete was determined using ACI 318-14 (ACI 2014). Winfrith material model does not account for post-peak compression softening. This issue was addressed by calibrating the maximum principal strain of concrete, after which elements are removed from the model (i.e. element erosion). The maximum principal strain for element removal was calibrated to be 0.04 (Epackachi and Whittaker 2018). Buckling of reinforcement was not considered in the model.

Reinforcing bars were modeled explicitly using piecewise linear plasticity material model (MAT024 in LS-DYNA). Piecewise linear plasticity model can account for fracture of reinforcing bars by limiting the accumulated plastic strain based on the stress-strain behavior of bars. Stress-strain relationship of reinforcing bars was extracted from Pilakoutas and Elnashai (1995).

Reinforcing bar beam elements and concrete continuum elements shared duplicate nodes, assuming a prefect concrete reinforcing bar bond. Foundation and cap beam were assumed linear-elastic. Cyclic lateral displacements were applied through the cap and the bottom face of foundation was restrained for all displacements and rotations. More information on materials used and modeling approach can be found elsewhere (Basereh et al.).

Comparison of FEA and experimental results

Figure 2 shows the comparison of force-displacement relationships from finite element analysis and experimental program. In general, FEA predicted the force-displacement results with reasonable accuracy. For the last two cycles of loading (drift ratios of 1.67% and 1.8%), lateral strength of the FEA was almost 20% lower than that of experimental results. This can be attributed to the simplified, trilinear idealization of stress-strain behavior of reinforcing bars used in models as reported by Pilakoutas and Elnashai (1995). Fracture of reinforcing bars was observed in the FEA but not in the experimental program.

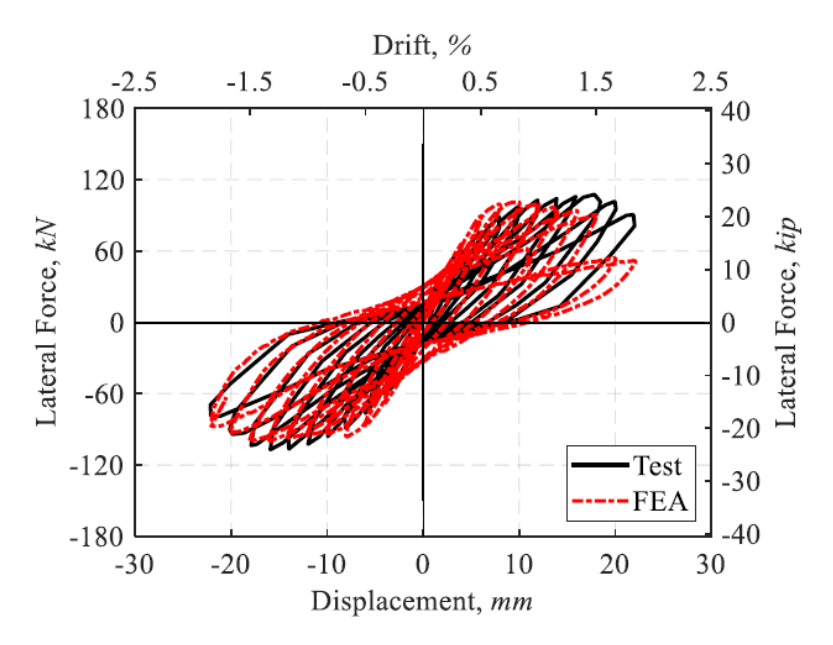


Figure 2. Force-displacement from FEA and experimental program

RETROFITTED RC WALLS

The proposed retrofit solution is a combination of weakening and self-centering. Weakening is performed by cutting the entire concrete and a portion of vertical reinforcing bars at the base. Three distinct non-straight cut shapes, namely, trapezoidal (shear-key type), circular and triangular, were considered to understand the effect of cut shape on horizontal shear and global response of the wall. Self-centering is ensured by adding external unbonded post-tensioned tendons to the wall.

Energy dissipation of the proposed retrofit solution is provided by the vertical reinforcement bars that are left uncut.

For the wall under consideration (SW6), only the outermost layer of the vertical reinforcing bars was cut. This left the retrofitted wall with 56% of reinforcing bar area of the pre-retrofit wall. This reinforcement amount is consistent with the recommendation for post-tensioned rocking walls that states that the amount of vertical reinforcement should be at least 50% of that of an equivalent cast-in-place cantilever wall (Kurama 2002). Reinforcement area can also be determined per recommendations of ACI ITG 5.1-07 (ACI ITG 2007) for the relative energy dissipation ratio, which is defined by the ratio of the area under a force-displacement hysteresis loop for a given cycle to the area of the circumscribing parallelogram defined by the initial stiffness and the peak resistance of the cycle.

The amount of initial post-tensioning force could be adjusted such that: first, the contribution of post-tensioning to the flexural resistance is larger than the contribution of uncut reinforcing bars to ensure sufficient self-centering (ACI ITG 2007), second, desirable lateral strength is obtained, and third, the post-tensioning strands yield when the wall reaches its maximum displacement capacity. For wall SW6, the amount of initial post-tensioning force was set to $0.11A_gf'c$, where A_g is the gross cross sectional area of the wall and f'c is the uniaxial compressive strength of concrete. Two strands (i.e. one strand on each side of the wall) initially post-tensioned to $0.5F_{py}$ were placed at the mid-length of the wall. Here, F_{py} denotes the yield strength of the post-tensioning strands. ACI 318-14 (ACI 2014) recommends taking yield strength of post-tensioning strands as 90% of the ultimate strength. The cross-sectional area of each strand was 93 mm² (0.144 in²).

Shear wall base cut shapes

The base lengths of the trapezoidal, semi-circular and triangular cut shapes were set to 400 mm (15.7 in.). For the trapezoidal (shear-key type) base cut, the height-to-length ratio and the angle of shear key with respect to the vertical axis was set to 0.1 and 25 degrees, respectively, as shown in **Figure 3(a)** per recommendations of fib (fib 2008). The length of the shear-key was adjusted such that the predicted neutral axis was within the flat portion of the wall base and not within the shear key. **Figure 3** shows the layout of the retrofitted walls together with the cross-section at the base.

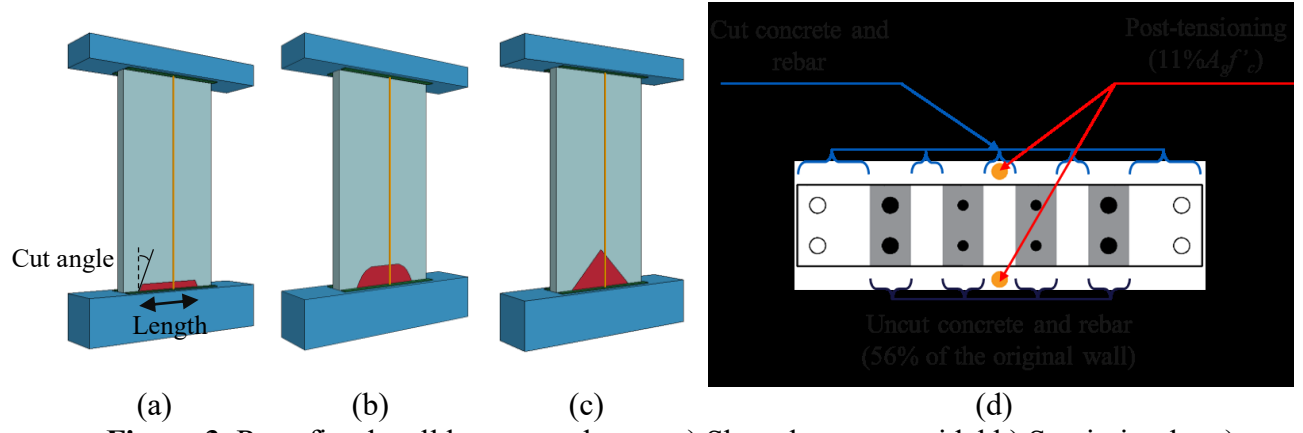


Figure 3. Retrofitted wall base cuts shapes: a) Shear-key trapezoidal b) Semi-circular c) Triangular, and d) wall base cross section

FEA of retrofitted walls

Validated FEA of the pre-retrofit wall was used to implement the retrofit method. To model post-tensioning strands, cable discrete beam material (MAT071 in LS-DYNA) was used. Cable discrete beam is an elastic material with zero tensile stiffness. Since yielding of strands is not considered, strand stresses should be checked to ensure that yield strength is not exceeded. Modulus of elasticity of strands was set to 196,500 MPa (28,500 ksi) per ACI 318-14 (ACI 2014) and strands were connected to the cap and foundation through rigid plates to prevent large deformations and instabilities at anchorages.

To simulate the base cut and the consequent rocking behavior, shared nodes of the wall and the foundation at wall base were detached. A mortar-based surface-to-surface hard contact was defined between the wall and foundation faces. The friction coefficient was set to 0.6 as this is within the range recommended by ACI 318-14 (ACI 2014) and ACI ITG 5.1-07 (ACI ITG 2007).

Three cut shapes (trapezoidal (shear-key type), circular, and triangular) were investigated. FEA results of the post-retrofit walls were compared to those of the pre-retrofit wall in terms of four parameters of interest: relative energy dissipation ratio, lateral strength, residual drift, and secant stiffness per cycle. ACI ITG-5.1-07 and 5.2-09 (ACI ITG 2007; ACI ITG 2009) require relative energy dissipation ratio of post-tensioned rocking walls to exceed 0.125. Residual drift was defined as the drift ratio at zero force for each cycle. Secant stiffness was defined as the lateral force to displacement ratio at the maximum displacement for each cycle. All reported results are the average values of all cycles in the positive and negative displacement direction unless otherwise stated.

In order to investigate the effectiveness of the proposed retrofit method, crack patterns and principal strain contour plots of pre- and post-retrofit walls were compared. Furthermore, to investigate the contribution of rocking, shear, and flexure to the global response of the walls, total deformation of the wall was decomposed to its components. Deformation decomposition of the pre- and post-retrofit walls were then compared.

COMPARISON OF PRE- AND POST-RETROFIT WALLS

Figure 4 compares the hysteretic force-displacement response of the pre- and post-retrofit walls for various base cut shapes. Trapezoidal (shear-key type), semi-circular, and triangular base cut shapes were considered. All base cut shapes led to sufficient energy dissipation capacity since they provided more than the minimum required relative energy dissipation ratio per ACI ITG 5.1-07 (ACI ITG 2007).

Figure 5 compares pre- and post-retrofit walls in terms of parameters of interest. Retrofitted walls with trapezoidal, semi-circular and triangular cut shapes resulted in 78%, 86%, and 74% lateral strength compared to the pre-retrofit wall, averaged over all loading cycles, respectively. The average residual displacement ratio of retrofitted walls to the original wall varied between 0.69 to 0.86. Among walls with various base cut shapes, the wall with the semi-circular cut had the least residual displacement.

Secant stiffness of all retrofitted walls was lower than that of the pre-retrofit wall. The secant stiffness ratios averaged over all cycles of loading, of retrofitted walls to the original wall were 0.78, 0.87, and 0.71 for trapezoidal, semi-circular, and triangular base cut shapes, respectively.

Crack patterns and principal strain contour plots

Figure 6 compares principal compression and tension strain contours at drift ratio of 1.8% (drift ratio associated with failure of the pre-retrofit wall) for pre- and post-retrofit walls. Solid black lines and white regions represent tensile cracks and eroded elements, respectively. For post-retrofit walls, principal compression strain contours reveal that, in general, crushing of concrete (i.e. area of red region) was less pronounced compared with the pre-retrofit wall and was more concentrated below or at the cut level. Under tension, cracking was limited to areas near the base cut of post-retrofit walls. The number of cracked finite elements in post-retrofit walls were fewer than the ones in pre-retrofit wall. Among all retrofitted walls, retrofitted wall with the circular base cut was the best in limiting both tensile cracking and compressive crushing of concrete elements.

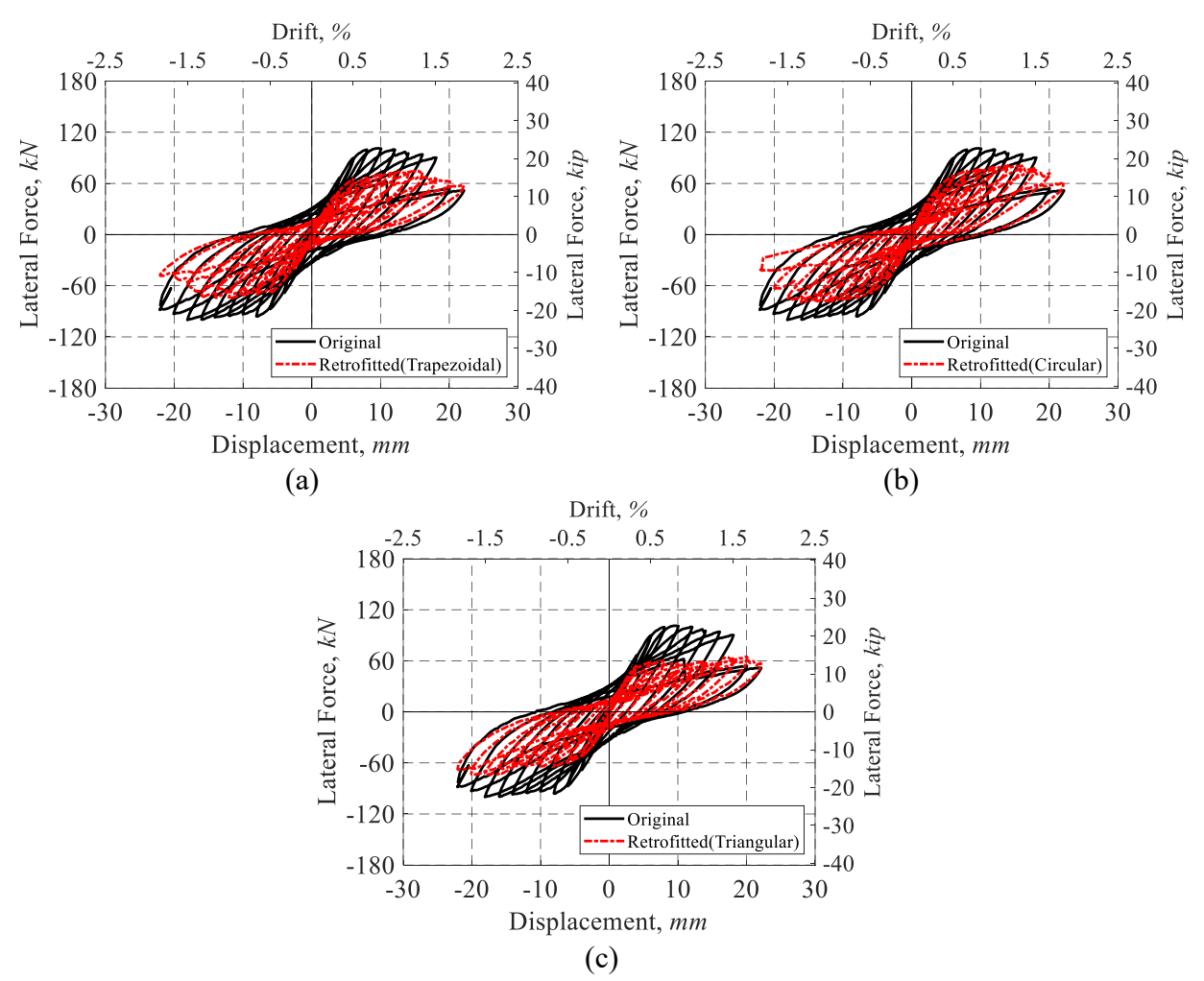


Figure 4. Comparison of pre- and post-retrofit walls in terms of force-displacement relationships a) Trapezoidal b) Circular c) Triangular cut shapes

Deformation decomposition

Deformations were decomposed into their components to investigate the contribution of each component to the total deformation. For the pre-retrofit wall, only flexural and shear deformations were considered. To determine flexural deformation, vertical strain at edges of the wall were extracted from the FEA at different wall heights. Assuming linear strain distribution along the length of the wall, curvature was calculated from vertical strains and integrated twice across the wall height to find the flexural displacement. Shear displacement was indirectly calculated by subtracting the flexural displacement from the total imposed lateral displacement.

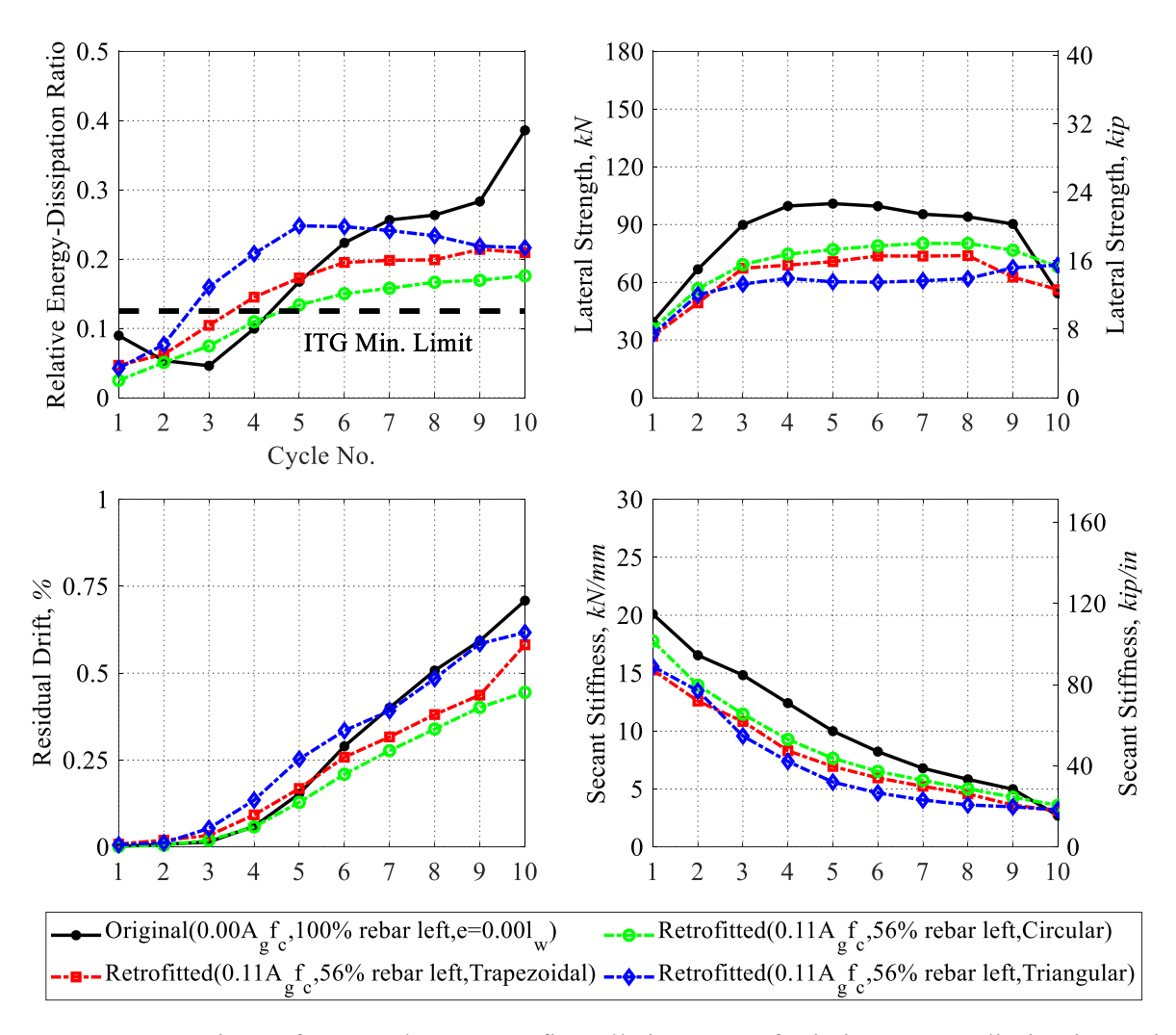


Figure 5. Comparison of pre- and post-retrofit walls in terms of relative energy dissipation ratio, lateral strength, residual drift and secant stiffness

For the retrofitted walls, total displacement is composed of recoverable (i.e. rocking) and partially or fully irrecoverable (i.e. sliding, flexural, and shear) deformations. Across the wall height between the foundation top surface and the top of the wall base cut shape (i.e. the top side of trapezoid, the top of the semi-circle and the top corner of triangle), rocking and sliding were

assumed to govern displacements. For the rest of the wall height (i.e. from the top of the cut and upward), sliding, flexure, shear and rocking displacements were considered.

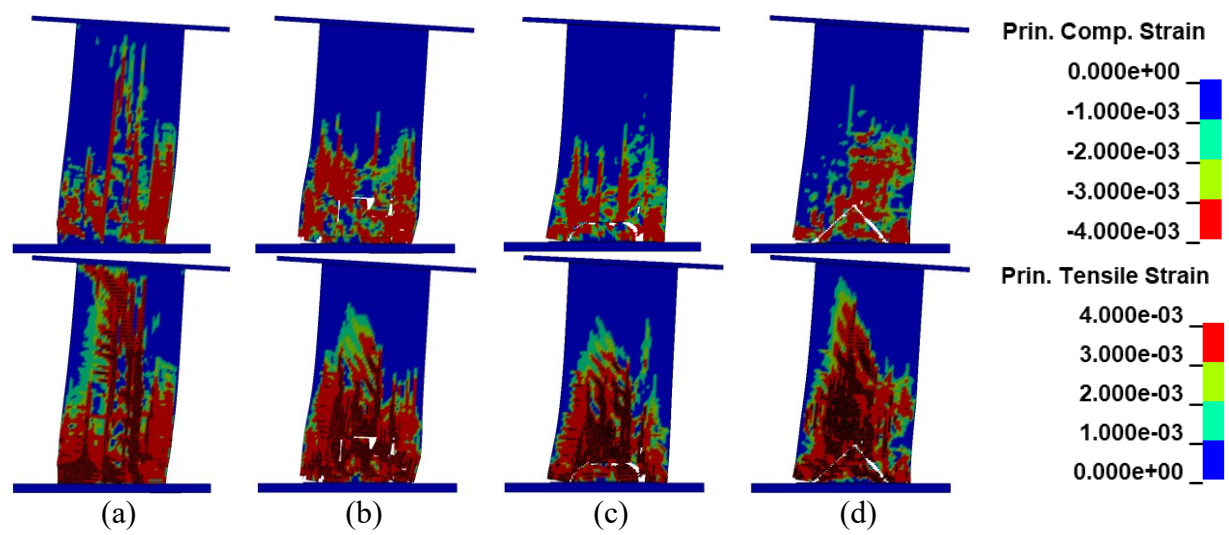


Figure 6. Principal strain contours for a) Pre-retrofit wall and post-retrofit walls with b) Trapezoidal c) Circular and d) Triangular base cuts at 1.8% drift ratio

Rocking (rigid body) deformation was determined by monitoring the uplift of the rocking edge of the walls and calculating the lateral deformation generated by this rigid body, uplift deformation. Sliding deformation at the wall base was found by tracking the horizontal displacement at the base of the wall in FEA. Note that, to estimate sliding deformations more accurately, the horizontal component of rocking displacement has to be subtracted from the sliding deformation. This component is expected to be small due to small angles of rocking and was neglected for simplicity. Flexural deformation was calculated using curvature following the same procedure used for the original wall. Shear deformation was calculated by subtracting the sum of rocking, sliding and flexure deformations from the total imposed displacement. **Figure 7** shows deformation decomposition of pre- and post-retrofit walls.

Rocking deformation was the largest type of deformation in retrofitted walls and was nearly half the total displacement. Contribution of flexural deformation to the global response was negligible since the upper part of the walls (i.e. parts higher than cut level) mostly remained elastic. Retrofitted wall with the trapezoidal base cut outperformed walls with other base cut shapes in controlling the sliding deformation as sliding was limited to less than 2 mm (0.08 in.). Sliding deformation was 6.3 mm (0.25 in.) and 4.6 mm (0.18 in.) for retrofitted walls with circular and triangular cut shapes, respectively. Contribution of shear deformation to the global response was reduced by 44%, 76%, and 53% with respect to the pre-retrofit wall for retrofitted walls with trapezoidal, semi-circular, and triangular base cut shapes, respectively.

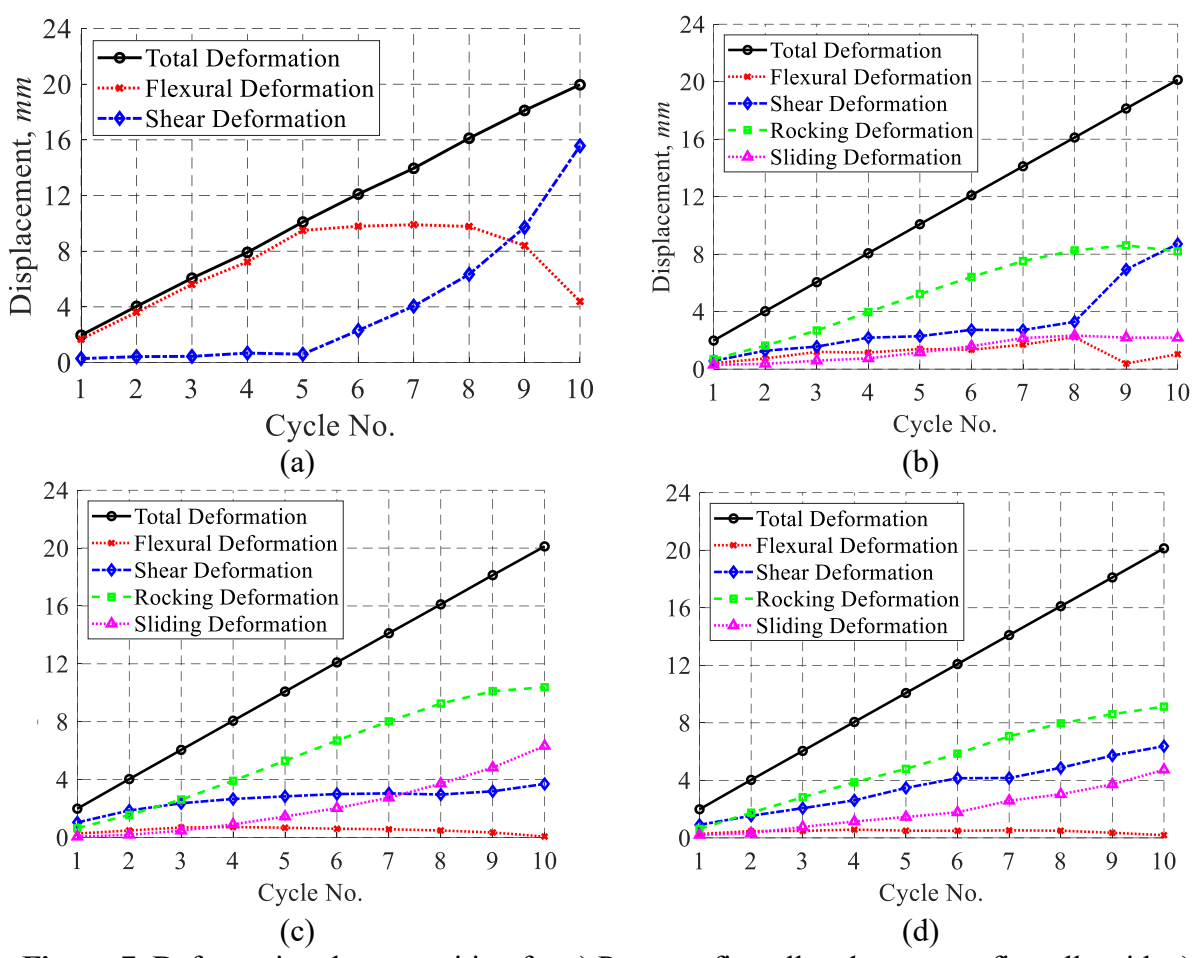


Figure 7. Deformation decomposition for a) Pre-retrofit wall and post-retrofit walls with a) Trapezoidal b) Circular c) Triangular cut shapes

CONCLUDING REMARKS

This study investigated the possibility of converting a non-ductile cantilever cast-in-place RC wall to a self-centering, rocking wall as a retrofit. Retrofitted walls with various base cut shapes (shear-key type trapezoidal, semi-circular, and triangular) were considered to minimize shear sliding at base. It was shown that combining selective weakening and self-centering as a retrofit solution resulted in lower lateral strength, residual displacement, and secant stiffness. Relative energy dissipation ratio was used as a measure to ensure that retrofitted walls can dissipate sufficient energy. Main conclusions drawn from the study are as follows:

- Flexure-shear response of a non-ductile cast-in-place RC shear wall was transformed into a
 more desirable response that includes rocking displacements, limiting residual
 displacements and minimizing damage to the wall
- Contribution of shear to the total deformation decreased by up to 76% for the post-retrofit wall with a semi-circular base cut shape compared to pre-retrofit wall.
- Trapezoidal (Shear-key type) wall base cut shape controlled the sliding shear more efficiently than other base cut shapes.

- Circular shape wall base cut shape had the least contribution from shear and consequently, had the least tensile cracking and compressive crushing among different cut shapes considered.
- The wall base cut shape did not influence lateral strength considerably.

ACKNOWLEDGMENTS

This material is based upon work supported by the National Science Foundation under grant No. 1663063. Any opinions, findings, and conclusions or recommendations expressed in this material are those of the authors and do not necessarily reflect the views of the National Science Foundation.

REFERENCES

- Aaleti, S., and Sritharan, S. (2009). "A simplified analysis method for characterizing unbonded post-tensioned precast wall systems." *Eng. Struct.*, 31(12), 2966-2975.
- Aaleti, S., and Sritharan, S. (2011). "Performance verification of the prewec concept and development of seismic design guidelines." Iowa State University,
- ACI (American Concrete Institute). (2014). "Building code requirements for structural concrete (ACI 318-14): Commentary on building code requirements for structural concrete (ACI 318R-14)" ACI 318-14, Farmington Hills, MI.
- ACI ITG (American Concrete Institute). (2007). "Acceptance criteria for special unbonded post-tensioned precast structural walls based on validation testing" *ACI ITG-5.1-07*, Farmington Hills, MI.
- ACI ITG (American Concrete Institute). (2009). "Requirements for design of a special unbonded post-tensioned precast shear wall satisfying ACI ITG-5.1 and commentary" *ACI ITG-5.2-09*, Farmington Hills, MI.
- Basereh, S., Okumus, P., and Aaleti, S. "Reinforced concrete shear walls retrofitted using weakening and self-centering: Numerical modeling." *J. Struct. Eng. (under review)*.
- Bruneau, M., Kenarangi, H., and Murphy, T. P. (2018). *Contribution of steel casing to single shaft foundation structural resistance*, NCHRP Research Rep. 872, Washington, DC: Transportation Research Board.
- Epackachi, S., and Whittaker, A. S. (2018). "A validated numerical model for predicting the inplane seismic response of lightly reinforced, low-aspect ratio reinforced concrete shear walls." *Eng. Struct.*, 168, 589-611.
- fib (federation internationale du beton). (2008). "Fib bulletin 43: Structural connections for precast concrete buildings"
- fib (federation internationale du beton). (2013). "Fib model code for concrete structures 2010"
- Henry, R. (2011). "Self-centering precast concrete walls for buildings in regions with low to high seismicity." Ph.D. Dissertation, University of Auckland, Auckland, New Zealand.
- Henry, R. S., Aaleti, S., Sritharan, S., and Ingham, J. M. (2010). "Concept and finite-element modeling of new steel shear connectors for self-centering wall systems." *J. Eng. Mech.*, 136(2), 220-229.
- Holden, T., Restrepo, J., and Mander, J. B. (2003). "Seismic performance of precast reinforced and prestressed concrete walls." *J. Struct. Eng.*, 10.1061/(ASCE)0733-9445(2003)129:3(286), 286-296.

- Ireland, M., Pampanin, S., and Bull, D. "Experimental investigations of a selective weakening approach for the seismic retrofit of rc walls." *Proc.*, *New Zeal. Soc. Earthquake Eng. 2007 Annual Conf.*
- Kam, W., and Pampanin, S. "Selective weakening techniques for retrofit of existing reinforced concrete structures." *Proc.*, 14th World Conf. on Earthquake Engineering (14WCEE).
- Kam, W., and Pampanin, S. (2010). "Experimental and numerical validation of selective weakening retrofit for existing non-ductile rc frames." *Improving the seismic performance of existing buildings and other structures*, 706-720.
- Kam, W. Y., and Pampanin, S. (2011). "The seismic performance of rc buildings in the 22 february 2011 christchurch earthquake." *Struct Concrete*, 12(4), 223-233.
- Kurama, Y. (2002). "Hybrid post-tensioned precast concrete walls for use in seismic regions." *PCI J.*, 47, 36-59.
- Kurama, Y., Sause, R., Pessiki, S., and Lu, L.-W. (1999). "Lateral load behavior and seismic design of unbonded post-tensioned precast concrete walls." *Struct. J.*, 96(4), 622-632.
- Kurama, Y. C. (2000). "Seismic design of unbonded post-tensioned precast concrete walls with supplemental viscous damping." *Struct. J.*, 97(4), 648-658.
- LSTC. 2017. Ls-dyna keyword user's manual, version 971 R 9.0, Livermore, CA, Livermore Software Technology Corporation.
- Nakaki, S., Stanton, J., and Sritharan, S. (1999). "Overview of the presss five-story precast test building." *PCI J.*, 44, 26-39.
- Nazari, M., Sritharan, S., and Aaleti, S. (2017). "Single precast concrete rocking walls as earthquake force-resisting elements." *Earthq. Eng. & Struct. Dyn.*, 46(5), 753-769.
- Pampanin, S. (2006). "Controversial aspects in seismic assessment and retrofit of structures in modern times: Understanding and implementing lessons from ancient heritage." *New Zeal. Soc. Earthquake Eng.*, 120-133.
- Perez, F. J., Pessiki, S., and Sause, R. (2004). "Lateral load behavior of unbonded post-tensioned precast concrete walls with vertical joints." *PCI J.*, 49(2).
- Pilakoutas, K., and Elnashai, A. (1995). "Cyclic behavior of reinforced concrete cantilever walls, part i: Experimental results." *ACI Struct J*, 92(3), 271-281.
- Priestley, M. N., Sritharan, S., Conley, J. R., and Pampanin, S. (1999). "Preliminary results and conclusions from the presss five-story precast concrete test building." *PCI J.*, 44(6), 42-67.
- Priestley, M. N., and Tao, J. R. (1993). "Seismic response of precast prestressed concrete frames with partially debonded tendons." *PCI J.*, 38(1), 58-69.
- Rahman, A. M., and Restrepo, J. I. (2000). "Earthquake resistant precast concrete buildings: Seismic performance of cantilever walls prestressed using unbonded tendons." University of Canterbury, Christchurch, New Zeland
- Restrepo, J. I., and Rahman, A. (2007). "Seismic performance of self-centering structural walls incorporating energy dissipators." *J. Struct. Eng.*, 10.1061/(ASCE)0733-9445(2007)133:11(1560), 1560-1570.
- Sharma, S., and Aaleti, S. "A study on residual drift and concrete strains in unbonded post-tensioned precast rocking walls." *Proc., Proceedings of the... Canadian Conference on Earthquake Engineering*.
- Smith, B., and Kurama, Y. (2014). "Seismic design guidelines for solid and perforated hybrid precast concrete shear walls." *PCI J.*, 59(3), 43-59.

- Smith, B. J. (2012). "Design, analysis, and experimental evaluation of hybrid precast concrete shear walls for seismic regions." Ph.D. Dissertation, University of Notre Dame, Notre Dame, Indiana.
- Smith, B. J., Kurama, Y. C., and McGinnis, M. J. (2010). "Design and measured behavior of a hybrid precast concrete wall specimen for seismic regions." *J. Struct. Eng.*, 137(10), 1052-1062.
- Sritharan, S., Aaleti, S., Henry, R. S., Liu, K.-Y., and Tsai, K.-C. (2015). "Precast concrete wall with end columns (prewec) for earthquake resistant design." *Earthq. Eng. Struct. D.*, 44(12), 2075-2092.
- Sritharan, S., Aaleti, S., and Thomas, D. J. (2007). "Seismic analysis and design of precast concrete jointed wall systems."
- Twigden, K., and Henry, R. "Experimental response and design of o-connectors for rocking wall systems." *Proc., Structures*, Elsevier, 261-271.
- Twigden, K., Sritharan, S., and Henry, R. (2017). "Cyclic testing of unbonded post-tensioned concrete wall systems with and without supplemental damping." *Eng. Struct.*, 140, 406-420.
- Wallace, J. W. (2012). "Behavior, design, and modeling of structural walls and coupling beams—lessons from recent laboratory tests and earthquakes." *Int. J. Concr. Struct. M.*, 6(1), 3-18.
- Yang, C., and Okumus, P. (2017). "Ultrahigh-performance concrete for posttensioned precast bridge piers for seismic resilience." *J. Struct. Eng.*, 10.1061/(ASCE)ST.1943-541X.0001906, 04017161.
- Yang, C., Okumus, P., and Ren, R. (2019). "A hysteretic model for self-centering precast concrete piers with varying shear-slip between segments." *Eng. Struct.*, 188, 350-361.